Anisotropic electrical transport properties of a two-dimensional electron gas at $SrTiO_3-LaAlO_3$ interfaces

P. Brinks, W. Siemons, J. E. Kleibeuker, G. Koster, G. Rijnders, and M. Huijben'

Citation: Appl. Phys. Lett. **98**, 242904 (2011); doi: 10.1063/1.3600339
View online: http://dx.doi.org/10.1063/1.3600339
View Table of Contents: http://aip.scitation.org/toc/apl/98/24
Published by the American Institute of Physics

Fearful for the future of science?
Sign up for FREE FYI emails.
AIP | American Institute of Physics

Anisotropic electrical transport properties of a two-dimensional electron gas at $SrTiO_3-LaAlO_3$ interfaces

P. Brinks,[1] W. Siemons,[2] J. E. Kleibeuker,[1] G. Koster,[1] G. Rijnders,[1] and M. Huijben[1,a)]
[1]*Faculty of Science and Technology, MESA+ Institute for Nanotechnology, University of Twente, P.O. Box 217, 7500 AE Enschede, The Netherlands*
[2]*Materials Science and Technology Division, Oak Ridge National Laboratory, P.O. Box 2008, Oak Ridge, Tennessee 37831-6030, USA*

(Received 19 April 2011; accepted 24 May 2011; published online 15 June 2011)

Experimental evidence of strong in-plane anisotropy in electrical properties of the confined electron gas at the $SrTiO_3-LaAlO_3$ interface on top of $(LaAlO_3)_{0.3}(Sr_2AlTaO_3)_{0.7}$ substrates is provided by detailed transport measurements. Structured measurement geometries in multiple directions are used to show dependence of the sheet resistance with the in-plane angle θ, which is fitted with a sine function with a period of 180°. The carrier density remains constant and a directional dependence of the carrier mobility of more than one order of magnitude is determined with respect to the orientation of the unit cell height steps present at the $SrTiO_3-LaAlO_3$ interface. © *2011 American Institute of Physics*. [doi:10.1063/1.3600339]

The remarkable observation of a high-mobility electron gas at the interface between the band insulators $SrTiO_3$ (STO) and $LaAlO_3$ (LAO)[1] has been attributed to electronic reconstruction, where the polarity discontinuity across the polar/nonpolar interface results in an energetically unfavorable build-up of electric potential causing the transfer of electrons from the surface, across the LAO layer, into the STO conduction band above a threshold of 3–4 unit cells (u.c.) of LAO.[2] An additional STO capping layer prevents structural and chemical reconstructions at the LAO surface resulting in metallic behavior below this threshold, even down to a single LAO unit cell layer.[3,4] To date, experiments have indicated that next to this intrinsic doping by the electronic reconstruction, also extrinsic doping could exist, originating from vacancy defects[5–7] or cation intermixing.[8] The confinement of the charge carriers was demonstrated by the controlled presence or absence of electrical conductivity by using a STO (001) substrate, which was, respectively, TiO_2-terminated or SrO-terminated.[1,9]

Electrical transport at the conducting interface occurs in a confined, but finite, region of low-dimensionality. Assuming the presence of a real two-dimensional electron gas (2DEG) near the interface, the properties have to be influenced by the unit cell height steps separating the terraces on the STO (001) surface. These steps are caused by the miscut angle, present in all single crystal substrates. These ordered surface steps are expected to have a dramatic effect on the transport properties and, therefore, a clear anisotropic electrical behavior should be observed when a real 2DEG is present. Knowledge about anisotropic effects and degree of two-dimensionality is required for implementation of such conducting interfaces in devices. In the present study, we show the detailed analysis of the strong in-plane anisotropy of 2DEGs at the STO–LAO interface on top of $(LaAlO_3)_{0.3}(Sr_2AlTaO_3)_{0.7}$ (LSAT) substrates, which was recently shown to exhibit a conducting interface.[10] Using LSAT substrates enables structurization of samples with measurement geometries by a combination of photolithography and argon ion etching, without inducing substrate conductivity, which is very challenging on heterostructures grown on STO substrates. Additionally, STO layers deposited by pulsed laser deposition (PLD) have shown a lower dielectric constant compared to single crystal substrates.[11] This leads to reduced electrical screening, possibly resulting in even stronger confinement of the free charge carriers at the interface.

Epitaxial heterostructures of STO and LAO have been grown on LSAT (001) substrates. The crystal structure of LSAT is cubic with a lattice parameter of 3.868 Å,[12] which closely matches the (pseudo)cubic lattice parameters of STO (3.901 Å)[13] and LAO (3.791 Å).[14] Single crystal LSAT (001) substrates (Crystec, GmbH) with various miscut angles were annealed at a temperature of 1050 °C for 10 h under a flow of O_2 of ~ 150 ml/min. This anneal treatment resulted in a very smooth surface with well defined unit cell steps separating the individual terraces, as can be clearly seen in the atomic force microscopy (AFM) image in Fig. 1(b), which represents the surface morphology of a typical LSAT substrate. All terrace steps have a height difference of a single unit cell indicating the presence of a mainly single terminated surface, which is in good agreement with previous studies reporting a surface with $>90\%$ $AlO_{2-\delta}/TaO_{2-\delta}$ termination after annealing.[15]

The STO–LAO heterostructures were fabricated by PLD with *in situ* reflection high-energy electron diffraction (RHEED) control of the growth process. Single crystal STO and LAO targets were ablated at a laser fluence of ~ 1.3 J/cm^2 and a repetition rate of 1 Hz. The substrate was held at 850 °C during deposition of both layers. The STO layer was deposited at an oxygen pressure of ~ 0.1 mbar, to obtain properties equivalent to single crystal values, while for the LAO layer oxygen pressures between 10^{-4} and 10^{-6} mbar were used. RHEED intensity oscillations are clearly observed during growth of each individual layer indicating control on the unit cell scale due to the layer-by-layer growth mode [Fig. 1(a)]. Results are given for the growth of a 10 u.c. STO bottom layer and a 10 u.c. LAO top layer. After growth, the heterostructures were slowly cooled

a)Electronic mail: m.huijben@utwente.nl.

 © 2011 American Institute of Physics

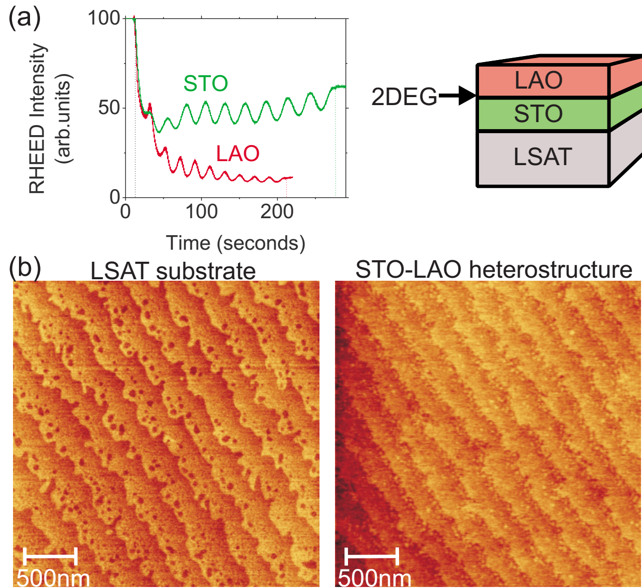

FIG. 1. (Color online) (a) RHEED specular spot intensity during layer-by-layer growth of 10 u.c. of STO and 10 u.c. of LAO at an oxygen pressure of, respectively, 0.1 mbar and 10^{-5} mbar. (b) Surface topography of an annealed LSAT single crystal substrate and a STO–LAO heterostructure deposited on LSAT.

to room temperature in the LAO deposition pressure of oxygen at a rate of 10 °C/min. The low level of surface roughness was confirmed by AFM analysis of the surface of the STO–LAO heterostructure [Fig. 1(b)], displaying smooth terraces separated by clear unit cell height steps similar to the surface of the initial LSAT substrate, indicating surface termination was maintained during deposition process.

Electrical transport properties were measured with a Quantum Design Physical Property Measurement System (PPMS) system and a flowcryostat. For detailed electrical anisotropy measurements, multiple measurement geometries, with a width and length of, respectively, 50 μm and 400 μm, at various angles were structured on the sample by a combined photolithography and argon ion-beam etching procedure. To determine sheet carrier density and mobility, multiple hall bar geometries, with a width of 40 μm and length of 160 μm, in different orientations have been structured.

The dependence of the transport properties on the oxygen deposition pressure for LAO growth between 10^{-4} and 10^{-6} mbar has been analyzed. For 10^{-5} and 10^{-6} mbar, the sheet resistance, sheet carrier density, fitted with a single band model, and carrier mobility are shown in Fig. 2. For samples with a deposition pressure of 10^{-4} mbar a much higher sheet resistance was measured at room temperature, which prevented accurately analyzing it at lower temperatures. However, a comparable sheet carrier density of $\sim 2 \times 10^{14}$ cm^{-2} at room temperature was determined for the total deposition pressure range. Figure 2 shows two different curves for each sample with values measured in two directions across the interface, perpendicular oriented to each other, i.e., parallel to the two different outer edges of the sample. A remarkable difference in sheet resistance of more than one order of magnitude is observed at low temperatures for these different directions [Fig. 2(a)]. The same difference can be observed in the carrier mobility [Fig. 2(c)] while a directional independent carrier density [Fig. 2(b)] is measured. These anisotropic effects have not been reported yet but the observed carrier density is in reasonable agreement with a previous study of LAO–STO interface growth on LSAT.[10]

Previous studies have demonstrated the formation of oxygen vacancies when growing the LAO–STO interface at low pressures on a STO (001) substrate.[1,5] This was supported by an increase in carrier density of three orders of magnitude. For our LAO–STO heterostructures on LSAT substrates this effect is not observed. A single STO layer deposited on LSAT remains insulating and the carrier density of the heterostructures remains constant down to a deposition pressure of 10^{-6} mbar. In addition to this, we can control the presence or absence of interface conductivity by controlling the surface termination of the STO layer. LAO layers grown directly on the deposited STO layer show conducting behavior, as expected for a TiO_2/LaO interface. However, fabrication of the other SrO/AlO_2 interface, by intermediate growth of a single SrO layer,[16] shows insulating behavior in good agreement with LAO–STO interfaces grown directly on STO substrates.[1,9]

The results of a more detailed study of the strong anisotropy in interface properties is shown in Fig. 3 for a heterostructure with a deposition pressure of 10^{-5} mbar for the LAO layer. The sheet resistance was measured in multiple directions across the sample with a measurement geometry as shown. For various temperatures the resistance is plotted as a function of the in-plane angle θ. Although clear anisotropic behavior is observed at all temperatures, the effect is especially strong at lower temperatures. Possible candidates causing anisotropic behavior are the crystallographic (100) and (010) orientations, which should be equal for cubic materials, and the direction of the terrace steps, i.e., the miscut orientation, which is limiting the two-dimensional nature of the interface. The periodicity of these two possibilities are, respectively, 90° and 180°. Since the observed anisotropy

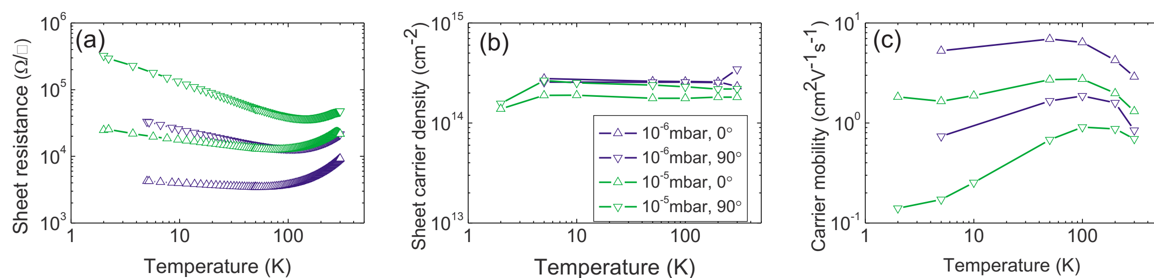

FIG. 2. (Color online) (a) Sheet resistance, (b) sheet carrier density, and (c) carrier mobility for a LAO layer deposited at 10^{-5} mbar and 10^{-6} mbar. Data are shown for two different measurement directions, perpendicular to each other, indicated by, respectively, Δ and ∇.

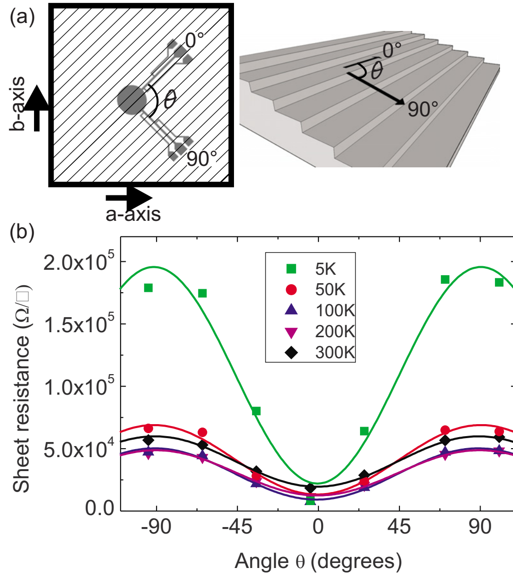

FIG. 3. (Color online) (a) Sample geometry with step and terrace structure and crystallographic a- and b-axes. (b) Resistance as a function of angle θ for various temperatures. Results are fitted with a sine function with a periodicity of 180°.

shows a periodicity of 180° the terrace steps at the interface seems to be the origin. To confirm the origin of the anisotropy we have used LSAT substrates with a miscut orientation of 45° with respect to a crystallographic axis to differentiate between the influence of the terrace steps, i.e., the miscut orientation, and the crystallographic axes [Fig. 3(a)]. From these measurements it is observed that the direction of lowest resistance corresponds to a direction parallel to the terrace steps, i.e., the highest carrier mobility is observed along the terraces [Fig. 3(b)].

If a model is assumed where the charge carriers within the 2DEG are strongly scattered by the unit cell height steps at the interface, a high mobility is expected parallel to the terrace steps and a low mobility is expected perpendicular to the terrace steps. A higher miscut would then result in an interface with a higher number of unit cell steps and therefore a stronger anisotropy. Anisotropy measurements for three different miscut angles at a temperature of 50 K are shown in Fig. 4. The angular dependence of the sheet conductance $(1/R_s)$ and carrier mobility at 50 K are plotted. The carrier mobility values are calculated, based on a constant carrier density of $\sim 2\times 10^{14}$ cm^{-2}, as determined previously. This overall lower mobility, as compared to STO–LAO interfaces grown on STO single crystals, could be explained by a higher defect density in the STO film, as compared to STO single crystals. These results cannot be explained by the simple intuitive model of carrier scattering at unit cell steps at the interface, as the strongest anisotropy is observed for the lowest miscut angle, i.e., lowest number of terrace steps. In order to further understand these observations, a more detailed model is required, which also takes into account the local meandering of the step edges.

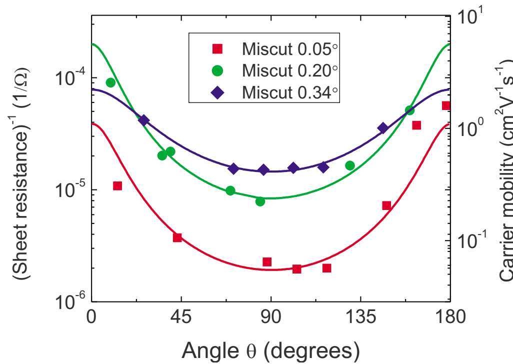

FIG. 4. (Color online) Sheet conductance $(1/R_s)$ and carrier mobility as a function of angle θ at a temperature of 50 K.

To conclude, we have observed strong anisotropic electrical transport properties for 2DEGs at the STO–LAO interface. The sheet carrier density is angular independent, whereas for the sheet carrier mobility differences of more than one order of magnitude were observed. It is shown that the angular dependence of the carrier mobility follows the miscut orientation of the LSAT substrate in which the highest and lowest mobilities are observed for, respectively, parallel and perpendicular directions to the terrace structure. This study demonstrates the importance of controlled surface preparation of the initial substrate in which the specific shape of terrace steps has dramatic effect on the final interface properties.

[1]A. Ohtomo and H. Y. Hwang, Nature (London) **427**, 423 (2004).
[2]S. Thiel, G. Hammerl, A. Schmehl, and J. Mannhart, Science **313**, 1942 (2006).
[3]M. Huijben, G. Rijnders, D. H. A. Blank, S. Bals, S. Van Aert, J. Verbeeck, G. Van Tendeloo, A. Brinkman, and H. Hilgenkamp, Nature Mater. **5**, 556 (2006).
[4]R. Pentcheva, M. Huijben, K. Otte, W. E. Pickett, J. E. Kleibeuker, J. Huijben, H. Boschker, D. Kockmann, W. Siemons, G. Koster, H. J. W. Zandvliet, G. Rijnders, D. H. A. Blank, H. Hilgenkamp, and A. Brinkman, Phys. Rev. Lett. **104**, 166804 (2010).
[5]A. Brinkman, M. Huijben, M. van Zalk, J. Huijben, U. Zeitler, J. C. Maan, W. G. van der Wiel, G. Rijnders, D. H. A. Blank, and H. Hilgenkamp, Nature Mater. **6**, 493 (2007).
[6]A. Kalabukhov, R. Gunnarsson, J. Börjesson, E. Olsson, T. Claeson, and D. Winkler, Phys. Rev. B **75**, 121404 (2007).
[7]W. Siemons, G. Koster, H. Yamamoto, W. A. Harrison, G. Lucovsky, T. H. Geballe, D. H. A. Blank, and M. R. Beasley, Phys. Rev. Lett. **98**, 196802 (2007).
[8]A. S. Kalabukhov, Y. A. Boikov, I. T. Serenkov, V. I. Sakharov, V. N. Popok, R. Gunnarsson, J. Börjesson, N. Ljustina, E. Olsson, D. Winkler, and T. Claeson, Phys. Rev. Lett. **103**, 146101 (2009).
[9]M. Huijben, A. Brinkman, G. Koster, G. Rijnders, and D. H. A. Blank, Adv. Mater. (Weinheim, Ger.) **21**, 1665 (2009).
[10]C. W. Bark, D. A. Felker, Y. Wang, Y. Zhang, H. W. Jang, C. M. Folkman, J. W. Park, S. H. Baek, H. Zhou, D. D. Fong, X. Q. Pan, E. Y. Tsymbal, M. S. Rzchowski, and C. B. Eom, Proc. Natl. Acad. Sci. U.S.A. **108**, 4720 (2011).
[11]H. C. Li, W. Si, R. L. Wang, Y. Xuan, and B. Liu, Mater. Sci. Eng., B **56**, 218 (1998).
[12]B. C. Chakoumakos, D. G. Schlom, M. Urbanik, and J. Luine, J. Appl. Phys. **83**, 1979 (1998).
[13]Y. A. Abramov, V. G. Tsirelson, V. E. Zavodnik, S. A. Ivanov, and I. D. Brown, Acta Crystallogr., Sect. B: Struct. Sci. **51**, 942 (1995).
[14]S. A. Hayward, F. D. Morrison, S. A. T. Redfern, E. K. H. Salje, J. F. Scott, K. S. Knight, S. Tarantino, A. M. Glazer, V. Shuvaeva, P. Daniel, M. Zhang, and M. A. Carpenter, Phys. Rev. B **72**, 054110 (2005).
[15]T. Ohnishi, K. Takahashi, M. Nakamura, M. Kawasaki, M. Yoshimoto, and H. Koinuma, Appl. Phys. Lett. **74**, 2531 (1999).
[16]G. Koster, G. J. H. M. Rijnders, D. H. A. Blank, and H. Rogalla, Appl. Phys. Lett. **74**, 3729 (1999).